Bifurcations and multiple-period soliton pulsations in a passively mode-locked fiber laser

J. M. Soto-Crespo
Instituto de Óptica, CSIC, Serrano 121, 28006 Madrid, Spain

Mélanie Grapinet and Philippe Grelu
Laboratoire de Physique de l'Université de Bourgogne, Unité Mixte de Recherche 5027 du Centre National de Recherche Scientifique, Boîte Postale 47870, 21078 Dijon, France

Nail Akhmediev
Optical Sciences Group, Research School of Physical Sciences and Engineering, The Australian National University, Canberra, Australian Capital Territory 0200, Australia

(Received 2 September 2004; published 13 December 2004)

We observed, numerically and experimentally, multiple-period pulsations of the soliton parameters in a passively mode-locked fiber laser. Pulsation periods can vary from a few to hundreds of round trips. Short and long period pulsations can appear in combination. The new periods in the soliton modulation appear at bifurcation points related to certain values of the cavity parameters.

DOI: 10.1103/PhysRevE.70.066612 PACS number(s): 42.65.−k, 47.20.Ky, 05.45.−a

I. INTRODUCTION

Laser systems generating ultrashort pulses [1–3] have a number of important applications in optics and telecommunications. The stability of the pulse generation from one round trip to another is one of the important qualities of such lasers. Any instability in the laser is considered to be detrimental for its use in applications. Indeed, if the characteristics of the output pulse start to deviate from the average, its use in an accurate technological device might stop its operation. The study of the instabilities becomes a crucial point when the configuration of the laser is designed. On the other hand, some instabilities lead to a regular change of the soliton parameters. This happens when periodic pulsations appear in the temporal evolution of the pulse. The pulse evolution with an additional periodicity can be stable itself. In this case, the pulsations can be observed in the output as periodic changes of the pulse shape and energy from one round trip to another. Then further devices can be designed based on these regular changes.

A laser cavity is a "cage" that forces pulses to evolve periodically with a period equal to the round-trip time. This is an internal periodicity and cannot be seen externally unless we monitor the pulse shape at several points of the cavity. When the pulse is monitored at a fixed point of the cavity, we can only observe its "macroevolution" at time scales longer than the round-trip time. It is usually assumed that a laser is in a stable regime of operation when the pulse returns to exactly the same profile after each round trip. This means that no macroevolution is present. The pulse might acquire an additional periodicity at some regimes determined by the parameters of the system. One of the transitions to periodic pulsations of a soliton is known as period doubling (tripling, etc.). Period doubling bifurcations have been found experimentally in various pulse generating laser systems. These include femtosecond solid-state lasers [4], fiber lasers [5–7], additive pulse mode-locked lasers [8], and nonlinear ring resonators [9].

Pulsating soliton solutions for the parameter averaged model of a laser have been studied in Ref. [10]. This model is based on the complex Ginzburg-Landau equation (CGLE) with constant parameters. It does not take into account the variation of the parameters in the cavity and the periods of the pulsating solutions in this model do not have a direct relation to the cavity length.

In the present work, we incorporated explicitly the cavity periodicity into the model. We have found that even in this case the pulse can acquire a periodic evolution that is not related to the round-trip time and can consist of many round trips. This "macroperiodicity" can exist independently or can be combined with other periodicities such as period doubling, tripling, etc. In the latter case the pulsations become quasiperiodic with two and more frequencies involved in this process. The frequencies can be commensurate or noncommensurate providing a rich variety of pulse outputs from the fiber laser.

II. THE MODEL

We model the fiber laser using the cubic-quintic complex Ginzburg-Landau equation with parameter management:

$$i\psi_z + \frac{D}{2}\psi_{tt} + |\psi|^2\psi + \nu|\psi|^4\psi = i\delta\psi + i\epsilon|\psi|^2\psi + i\beta\psi_{tt} + i\mu|\psi|^4\psi \tag{1}$$

where z is the distance that the pulse travels in the cavity (normalized to the cavity length), t is the retarded time, ψ is the normalized envelope of the field, D is the group velocity dispersion coefficient, δ is the linear gain-loss coefficient, $i\beta\psi_{tt}$ accounts for spectral filtering ($\beta>0$), $\epsilon|\psi|^2\psi$ represents the nonlinear gain which arises from saturable absorption, the term with μ represents, if negative, the saturation of the nonlinear gain, while the one with ν corresponds, also if negative, to the saturation of the nonlinear refractive index.

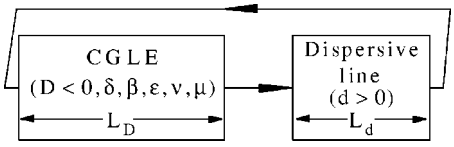

FIG. 1. Laser model used in the numerical simulations.

The laser cavity consists of several pieces of fiber, connecting elements and a mode-locking device. The properties of the media where the pulse propagates vary with the distance. Hence, the coefficients in Eq. (1) must be periodic functions of the distance z. Our aim is to show the existence of quasiperiodic limit cycles in the simplest model. Hence, we take the coefficients in Eq. (1) as periodic stepwise functions of z.

This technique for modeling the fiber laser can be called "parameter management." The term comes from the theory of "dispersion managed solitons" [11,12] which uses the nonlinear Schrödinger equation (NLSE) with stepwise coefficient in front of the second order derivative term. The periodic change of the group velocity dispersion induces evolution of the soliton profile that is usually chaotic but may become periodic provided the initial condition is chosen in a special way.

We use a similar approach for our laser system but instead of the nonlinear Schrödinger equation we use the cubic-quintic Ginburg-Landau equation with coefficients that are all periodic stepwise functions of z. Each period in this model naturally describes one round trip of the optical pulse. In contrast to the "dispersion managing" of the NLSE, the pulse evolution in our model does not depend generally on the initial conditions after a certain number of round trips. In the majority of the cases we use a sech-type profile to start the simulations with a single pulse. The pulse evolves into the solution provided it has the amplitude above a certain threshold given by the parameters of the system. If the amplitude of the initial condition is below this threshold, it decays and quickly vanishes.

The model is illustrated in Fig.1. The section of the erbium doped fiber together with the passive mode-locking element is modeled by the full CGLE equation where all the equation parameters are different from zero (see the left hand side box of this figure). The dispersion in this section of the cavity is taken to be normal ($D<0$) and the length of the section is L_D. The single mode fiber with anomalous dispersion ($D=d>0$) is modeled by the same equation with only the dispersive term taken into account (the right hand side box of this figure). The length of this fiber is denoted as L_d. The equation in this part is linear and therefore the only relevant parameter is the product (dL_d). The pulse profile is monitored every round trip at the end of this section unless specified otherwise.

As happens in dissipative systems, the solution does not depend generally on the initial condition (i.e., input pulse) after the pulse has propagated several round trips. In other words, any input pulse converges to a fixed stable profile or to a limit cycle quickly after the laser is "switched on." This happens for a certain range of values of the equation parameters for which the limit cycle is stable. Only these cases are of interest in our problem as well as for practical purposes. Only in a few cases, when bistability (or multistability) is present, the initial condition is important. The value of the parameters of the system determine the period of the pulsations. In particular, the period can be equal to two, three, etc., round trips rather than one. These phenomena are known as period doubling, tripling, etc., in the existing literature [5–8]. We have found pulsating behaviors with almost any integer number N of round trips as period. This observation requires a careful search for the proper values of the system parameters. Each additional frequency in the pulsations appears at some fixed values (bifurcation point) of the system parameters that we vary during simulations.

The model that we use is an approximation like any other. However, it takes into account the most important feature, namely, the round-trip periodicity of the effects suffered by the pulse during its propagation inside the laser cavity. As a result, it describes the soliton pulsation phenomena observed in experiments more accurately. As an alternative, we could use a lumped model in which certain devices, such as a mode locker or other, are introduced at a point rather than in an interval. The results we obtain will qualitatively be similar as soon as we take into account the round-trip periodicity explicitly in the model.

III. EXPERIMENTAL SETUP

We observed experimentally several of the simulated oscillatory behaviors. The experimental setup consists of a dispersion-managed mode-locked fiber ring laser similar to those used in Refs. 13 and 14. The fiber laser, which emits

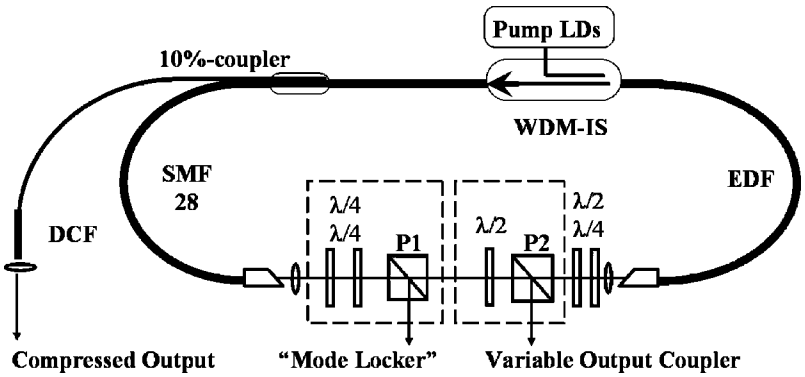

FIG. 2. Experimental setup.

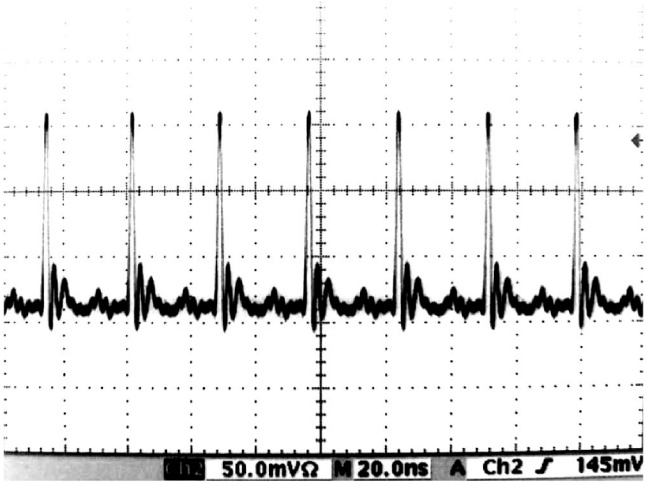

FIG. 3. Stable pulse train generation by the mode-locked fiber laser with a single soliton in each round trip.

ultrashort pulses at a wavelength of around 1.5 μm, is sketched in Fig. 2. The gain is provided by a 1.9-m-long, 1400-ppm erbium-doped fiber (EDF) that features normal chromatic dispersion $[D=-40\ (\mathrm{ps/nm})/\mathrm{km}]$. The pumping source consists of four wavelength-multiplexed laser diodes around 980 nm, providing a coupled power of up to 350 mW. The path-averaged cavity dispersion is adjusted with the use of an appropriate length of a SMF-28 fiber that has anomalous dispersion $[D=+16.5\ (\mathrm{ps/nm})/\mathrm{km}]$. A 50-cm-long open air section is used to insert polarization components. Due to the nonlinear polarization evolution that takes place along with propagation in the fibers, the transmission through the polarizer $P1$ is intensity dependent, and an appropriate adjustment of the preceding wave plates triggers the mode-locked laser operation. A polarization-insensitive optical isolator wavelength-division-multiplexed coupler and optical isolator (WDM-IS) ensures unidirectional lasing.

Two other optional outputs are implemented in the cavity, and may be used according to which type of experiment is performed. First, a second polarizer ($P2$), preceded by a half-wave plate, provides a convenient variable output coupler. We can use the half-wave plate to continuously tune the amount of cavity losses in a given range, so that oscillations can manifest accordingly. Second, a 10% fiber output coupler is inserted inside the cavity in order to splice a small length of dispersion-compensation fiber (DCF). This gives a convenient way to compress the chirped pulses that propagate in the cavity. Recording the optical autocorrelation from this fiber output is used to distinguish the doublet and triplet multisoliton complexes when the pulses are very close to each other. In the present work, the path-averaged dispersion is normal but very close to zero $[D\approx -2\ (\mathrm{ps/nm})/\mathrm{km}]$. The main attention is focused on the amount of energy carried by pulses at each round trip [denoted as Q in simulations, $Q=\int_{-\infty}^{\infty}|\psi(z,t)|^2dt$].

We record the output intensity from the 10% fiber output coupler with a fast InGaAs photodiode that is connected to a 500-MHz digital phosphor oscilloscope. At a pumping power of around 150 mW, fundamental mode locking is routinely achieved and can be stable for hours without the use of any external feedback. Due to the frequency chirping, the pulse duration is typically 1 ps at the open-air section outputs, and 150 fs at the compressed output port (see Ref. [14]). Intracavity energy of a single pulse is around 400 pJ. In a stable regime of laser operation, monitoring the output intensity displays the amplitude peaks that repeat at the cavity fundamental frequency of 36.6 MHz. The oscillogram for this regime is shown in Fig. 3.

IV. SHORT PERIOD PULSATIONS

We call "short period pulsations" those whose period is comparable with the round-trip time. When this period coincides with the round-trip time, the laser is in the stable regime of pulse generation, i.e., it produces exactly the same pulse each round trip. This regime is illustrated in Fig. 4(a). It shows the soliton peak amplitude versus the energy Q of the pulse as it evolves one round trip inside the cavity. After each round trip the trajectory returns exactly to the initial point. The parameters of the simulation are written inside the figure.

The curve is a closed single loop that shows that soliton parameters change periodically repeating themselves after each round trip. The experimental equivalent of this dynamics is presented in Fig. 3. For any arbitrary initial soliton parameters, the trajectory is out of this loop but it converges to it in a number of round trips. Hence, the loop is a stable limit cycle according to the common terminology used in nonlinear dynamics theory. As in the rest of this paper, any transitory evolution needed to reach the solution from arbitrary initial conditions is removed from the plot in Fig. 4.

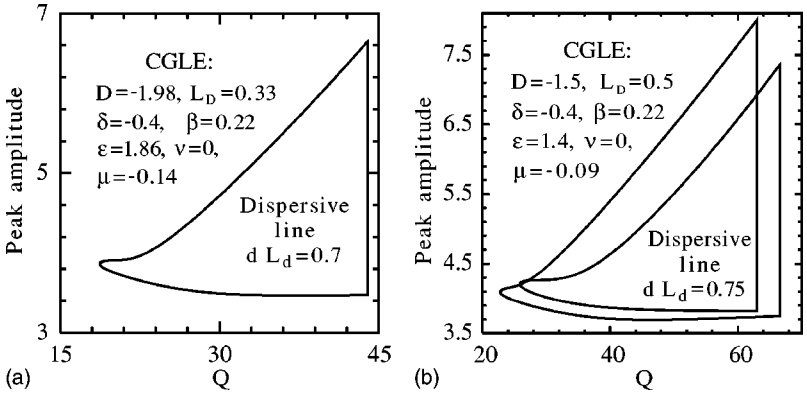

FIG. 4. Peak amplitude vs energy Q for (a) a period-1 solution as it evolves one round trip inside the cavity. The vertical part of this trajectory corresponds to the propagation during the purely dispersive stage. (b) Period doubled loop in passing the laser cavity twice.

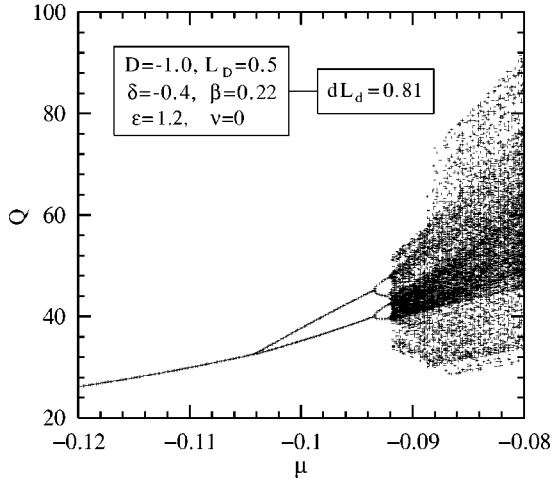

FIG. 5. Output energy Q monotored at the end of the amplifying stage as a function of μ. It shows a sequence of period doubling bifurcations in our parameter managed model of a fiber laser. The laser parameters are shown in the figure.

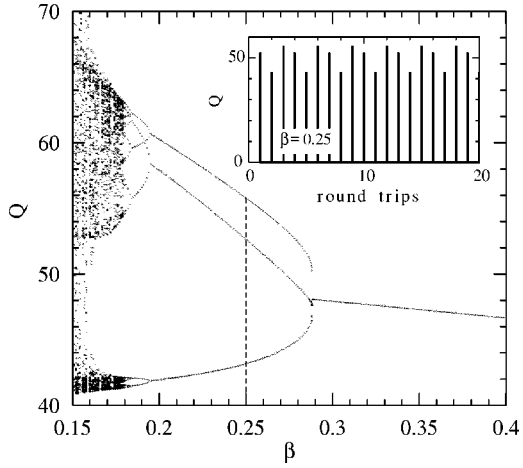

FIG. 7. Period tripling bifurcation when changing the parameter β. (Inset) Pulse energy versus the number of round trips for the period-3 solution at $\beta=0.25$ (indicated by a dashed line in the main figure). The parameters of the simulations, other than β, are shown in the inset in Fig. 6(a).

A similar loop can be constructed, if we choose any other soliton parameters, i.e., the width, *N*th order momentum of the pulse, etc. For any two of those parameters we obtain a two-dimensional projection of the limit cycle. If we use all of those parameters and construct a trajectory in the resulting infinite-dimensional space, we will have a periodic loop again. Hence, this is a limit cycle in an infinite-dimensional phase space.

The parameters of the system define the period of the pulsations. In particular, we can find the period being equal to two round-trip times rather than one. One of these cases is shown in Fig. 4(b). The parameters of our model that causes such transformation are shown in the figure. As a rule, the period-1 pulsations become unstable but the cycle with two loops becomes stable instead. This phenomenon is known as period doubling bifurcation.

In the example shown in Fig. 4, we changed several parameters in order to obtain period doubling. In many cases, we can vary only one of the parameters in the system to have a bifurcation or even a sequence of bifurcations. If we choose the gain saturation μ as a variable parameter we can also observe period quadrupling, i.e., the pulse repeats itself only after four round trips. In this case, both period-1 and period-2 solutions become unstable. The diagram showing the sequence of period doubling bifurcations is presented in Fig. 5. Period 4 appears at the value of $\mu \approx -0.093$. Further change of μ gives period-8 solutions and chaotic evolution of pulses at around $\mu=-0.092$. The whole sequence of period doubling bifurcations exists but cannot be resolved in the scale of Fig. 5. Similar evolution can be observed when we continuously change one of the other system parameters.

Another example of periodic behavior is shown in Fig. 6(a). It corresponds to a pulsating soliton evolution whose period covers three cavity round-trip times. The pulse energy versus the number of round trips is shown in the inset of Fig. 7. Each figure shows strict periodicity with the period being equal to three round trips.

After performing many numerical simulations, we are convinced that it is possible to find pulsating behavior with any integer number *N* of round trips. This requires a careful search for the values of the system parameters. Depending on the choice of the parameter that we use as a variable, the solutions might appear as a sequence of bifurcations such as period doubling bifurcations or we can get a more complicated sequence. In particular, the diagram with the period tripling bifurcation is shown in Fig. 7. In this case, when changing the spectral filtering parameter β, we have a transition directly to the period-3 solution rather than to period 2

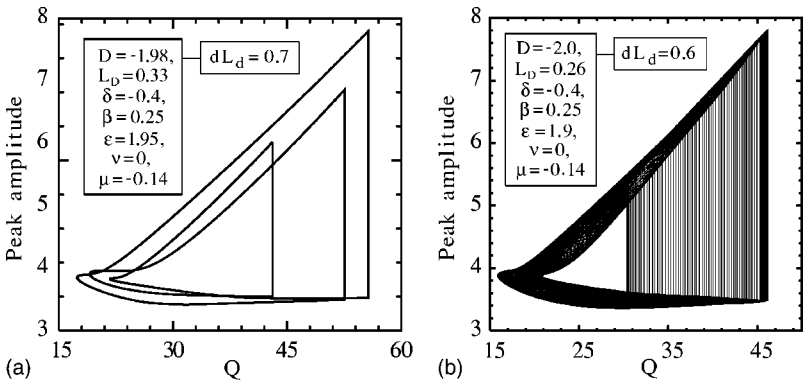

FIG. 6. (a) Period tripling loop obtained in passing the laser cavity three times. (b) Period-3 loop with an additional "long period" modulation in multiple passes through the laser cavity. The values of the parameters of the two simulations are shown in the insets.

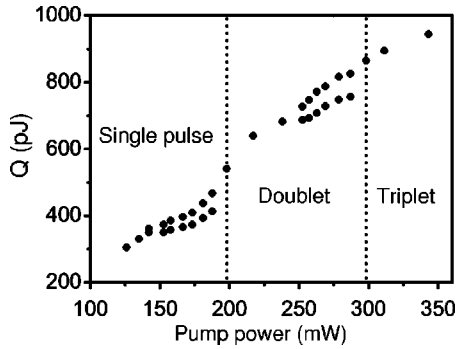

FIG. 8. Bifurcation diagram showing the formation of doublet and triplet multisoliton states in addition to period doubling (at $P \approx 140$ mW and $P \approx 240$ mW).

at the bifurcation point. The bifurcation occurs at $\beta \approx 0.288$. When further reducing the parameter β, we obtain the transition to the period-6 solution. Further reduction in β leads to chaotic solutions after a series of bifurcations with period multiplication.

The form of the bifurcation diagram depends on the trajectory in the parameter space that we choose for our simulations. In the two cases presented above, we fixed all the parameters except one, μ or β. This is the easiest way to change parameters in the simulations. Experimentally, changing the configuration might cause a simultaneous variation of several parameters. Then, the trajectory in the parameter space can be more complicated. Each route creates a specific bifurcation diagram.

Experimental observations

Once mode locking is achieved at a given pumping power and a given setting of waveplates, we have some latitude to vary one or several cavity parameters to observe changes in the dynamics of the output pulses. The change of the pump power and the orientation of the waveplates influences the coefficients δ, ϵ, and μ, leaving β and ν unchanged. However, the pump power variations influence these parameters in proportions different from the way when we change the orientation of the waveplates. As a result, the effects introduced in these two cases are different.

In the frame of the present paper, comparisons with theory and numerical simulations are consistent when only a single pulse is circulating in the cavity. For two or more pulses, we have to modify our model and take into account the gain saturation dependent on the total energy generated by the laser [15]. This is not done in the present work. We know from previous work [13,14] that multiple pulsing and the formation of multisoliton complexes can be favored in the cavity when the intracavity energy is increased. Multiple pulsing can be seen as a possible way of restoring the energy balance in the cavity and stabilizing the laser operation.

The change of the mode of the laser operation with increasing pump power is shown in Fig. 8. When the pumping power is increased to 140 mW, period-2 oscillations appear. These exist at higher power levels. However, at $P=200$ mW, instead of having more complex patterns of oscillations and chaos, a doublet soliton is formed, and period-2 oscillations disappear.

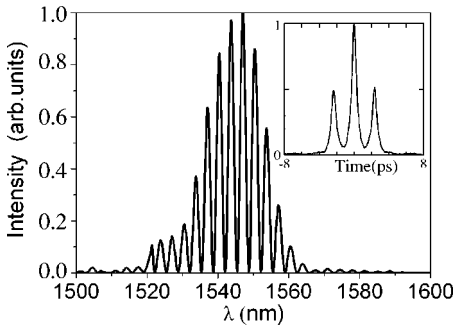

FIG. 9. Spectrum of soliton pair. The inset shows the optical autocorrelation function of the soliton pair.

The newly formed state can be analyzed using the recordings of its optical spectrum and autocorrelation trace. The stable soliton pair, or doublet, is characterized by highly contrasted fringes in its spectrum, whose interfringe distances are inversely proportional to the temporal separation of the two pulses, as measured by the autocorrelation trace.

Figure 9 presents the spectrum and, in the inset, the autocorrelation trace, of the doublet state. Further increase of the pumping power above 230 mW leads to another period-2 bifurcation. At higher power levels we observe the creation of an additional third pulse, namely, a stable multisoliton triplet is formed at around $P \approx 300$ mW. The spectrum of the triplet shows a characteristic fine fringe pattern (see Fig. 10). The autocorrelation function has five peaks rather than three (see the inset in Fig. 10).

The increase of the intracavity energy brings the instabilities described above. However, large instabilities are prevented by sharing the intracavity energy between several pulses that are bound together [17]. This observation of stabilization through additional pulse formation was also recently reported in Ref. [6], where a recursive simple model was given to explain that dynamic behavior.

In order to observe more complex dynamics associated with the circulation of a single pulse in the cavity, we have the latitude to vary different cavity settings. Indeed, once stable single pulse mode locking is obtained, we can vary the orientation of the mode-locking waveplates. This operation results in the modification of the whole nonlinear transmission function of the open-air section. This is different from

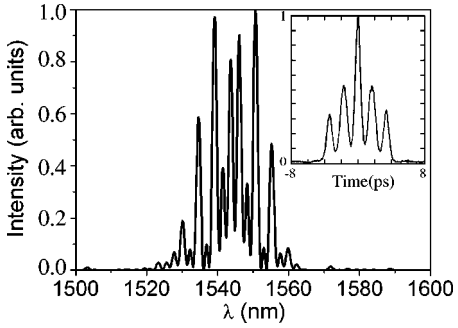

FIG. 10. The spectrum of soliton triplet. The inset shows the optical autocorrelation function of the soliton triplet.

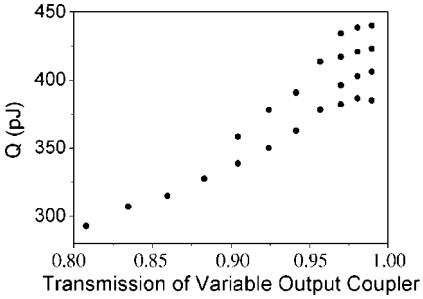

FIG. 11. Experimental bifurcation diagram revealing period-2 and period-4 dynamics.

the numerical simulations where a single parameter is varied at a time. In the experiment, we can also tune the amount of losses which is related to the orientation of the half wave-plate preceding polarizer $P2$. Starting from a stable (period-1) single pulse and the amount of 20% loss due to the variable output coupler, we reduce that amount and observe the sequence of period-2 and period-4 bifurcations that is represented in Fig. 11. The bifurcation points are clearly resolved at transmission values of around 0.9 and 0.97. We can see from this example that tuning the amount of losses is not equivalent to tuning the pumping power, as the dynamics involved can be quite different.

Dynamics with periods different from 2 and 4 can also be observed. Period-3 pulsations are one of the easily observed dynamics. Figure 12 shows an example of period-6 pulsations that appears in the sequence with the period tripling bifurcation. This observation is a qualitative analog of the solutions obtained for the values of β in the interval [$\approx$0.184, 0.196] in Fig. 7.

V. LONG PERIOD PULSATIONS

We call "long period pulsations" those pulsating solutions that have a period much longer than the round-trip time. As a rule, the period in this case is not an integer of the round-trip

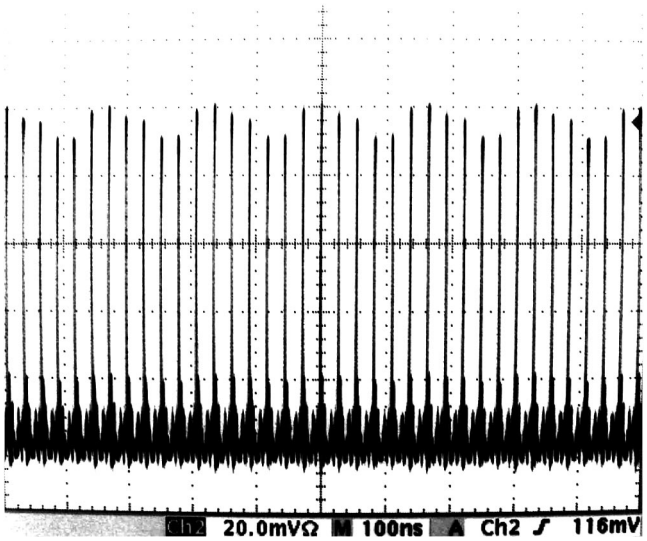

FIG. 12. Period-6 pulsations (experiment).

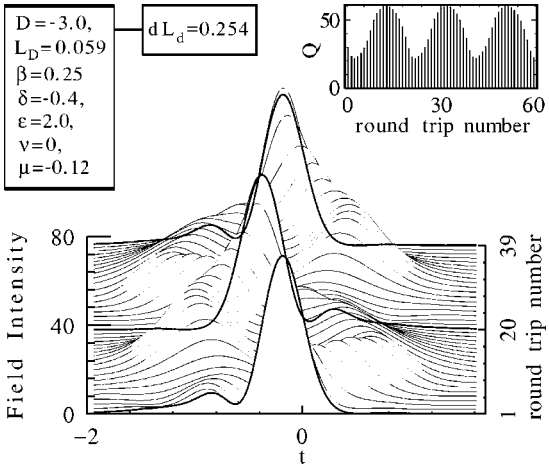

FIG. 13. An example of long period ($\approx$38 round trips) pulsations. The lower part shows the evolution of the pulse profile. Pulse profiles at $N=1$, 20, and 39 are plotted in thicker lines for the sake of comparison. The upper left inset shows the simulation parameters and the upper right one the pulse energy versus the round-trip number.

time although it can become commensurate to it with a careful adjustment of the system parameters. There are many types of long period pulsations. One example of such pulsations is shown in Fig. 13. The pulse is asymmetric at any particular value of z. As a result, it moves with a velocity that changes over a period. In addition, the pulse changes its profile continuously, which is also far from having a simple bell shape. It splits into two and rejoins again. In spite of such a complicated behavior, on average, the pulse keeps the same position in t. The total period of pulsations in this example is $N\approx 38$. The pulse changes its symmetry relative to the transformation $t\rightarrow -t$ after approximately 19 round trips. As a consequence, the energy Q plotted versus the number of round trips (see the right hand inset) shows the periodicity being $\approx$19.

The variety of possible pulsating solutions is enormous. We observed a multiplicity of such solutions in various regions of the parameter space. In this article, we restrict ourselves only to one particular example shown in Fig. 13. A complete study of the major properties of such solutions would require a separate publication. The pulse can change periodically its profile, chirp, and group velocity and oscillate back and forth relative to its average position in the moving frame of reference. We were able to reproduce all types of pulsating solutions that were obtained earlier in the continuous model [10,16]. That includes examples of "creeping" and "double creeping" solitons, etc. The period of pulsations that we observed in numerical simulations varied up to a few hundred round trips. The pulse energy modulation can also be changed in a wide range reaching the values of up to 60%.

It would be hard to observe all the features of the pulse transformation in z experimentally. The spectra and autocorrelation techniques are usually applied to the case of stationary pulses. When the pulse changes its parameters, its accurate characterization becomes a very difficult task. However, we can see the periodic changes of the pulse energy in the

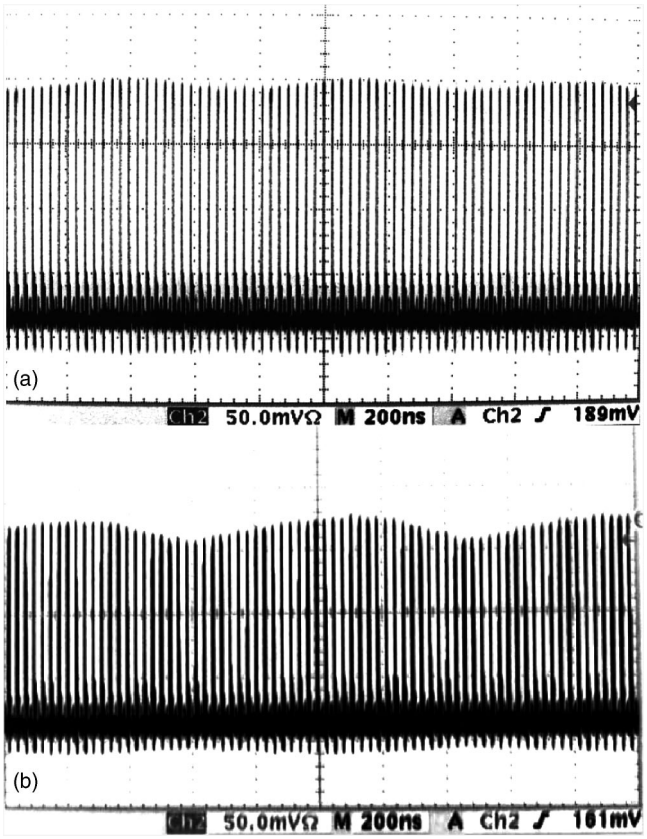

FIG. 14. Two examples of long period pulsations. (a) Pulsations with small soliton energy modulation and with the period ≈26 round trips. (b) Pulsations with a larger soliton energy modulation (the period ≈32 round trips).

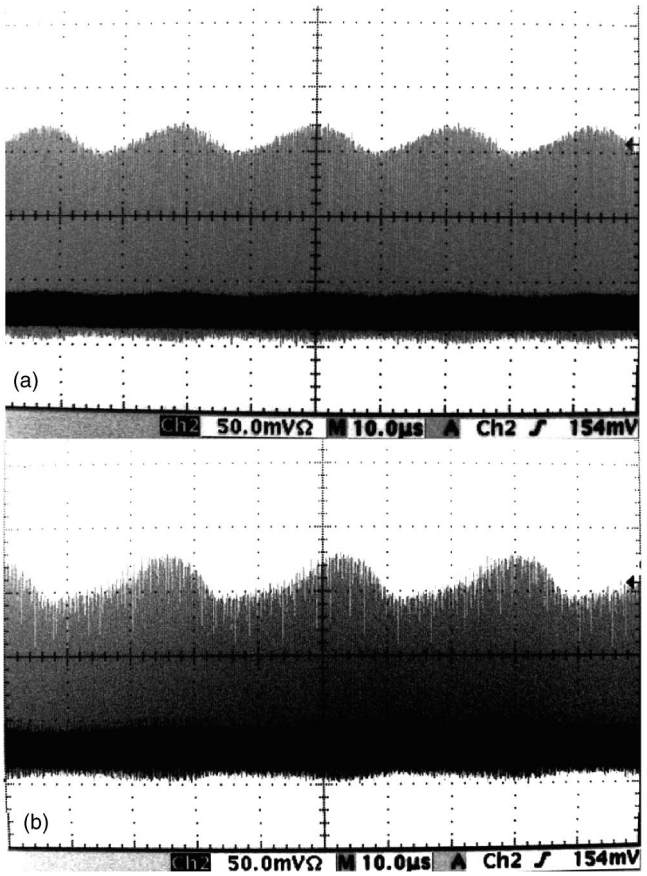

FIG. 15. Two examples of long period pulsations. (a) The period is around 815 round trips and (b) the period is around 910 round trips.

oscilloscope traces and these show undoubtedly that long period pulsations exist indeed.

Experimental observations

In order to observe long period pulsations in the experiment, we shift one of the four waveplates used to obtain mode locking. It affects the whole nonlinear loss function in the cavity. This way we can maintain single pulse mode locking, while achieving significant pulse changes from one round trip to the next. These changes are generally periodic. It turns out that rotating the mode-locking waveplates may result in the dramatic change from one type of periodic regime to another.

When the laser output features such amplitude modulations, no additional pulses are formed in the cavity and we are always dealing with a single pulse. Changing the parameters around the regime of stable mode locking (single pulse period 1), we obtain long period modulation of the output pulse energy. After entering this regime, the increase of the soliton energy modulation can be achieved either by increasing the pumping power or by a subsequent tuning of the mode-locking waveplates. When the soliton energy modulation is small, it appears as a sinusoidal modulation. This is illustrated by the recording in Fig. 14(a), which reveals period-26 pulsations. In the majority of the experimental arrangements, larger soliton energy modulations correspond to longer periods.

When the soliton energy modulation is high, it reveals more complicated nonsinusoidal evolution. This is illustrated by the oscillogram in Fig. 14(b). These results are in qualitative agreement with numerical simulations that show complicated but periodic behavior. Much longer periods, of the order of 1000 and longer, have been achieved in our experiments. Two examples are shown in Figs. 15(a) and 15(b). Comparing the two figures, we can see the transition from almost sinusoidal modulation to a modulation with more complicated structure.

Very large soliton energy modulations lead to the complete disruption of the single pulse mode-locking regime. Either the laser enters a multipulse regime of generation, or pulses in each round trip become so unstable that mode-locking stops and the laser enters a quasi-cw noisy regime of operation. However, the range of parameters where periodically modulated pulse generation exists is very large and comparable to the range where we have stable pulse generation.

VI. DOUBLE PERIODIC SOLITON PULSATIONS

Pulsations become complicated when two periods of oscillation are involved in the dynamics. A large variety of

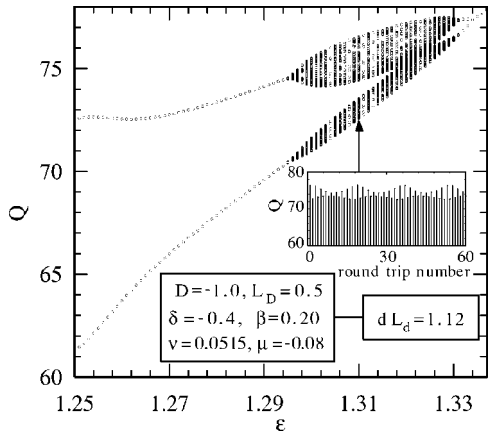

FIG. 16. The total soliton energy Q versus ϵ. The lower inset gives the values of other parameters used for the simulations. This diagram shows the period doubling bifurcation at $\epsilon \approx 1.332$. Bifurcations leading to additional long period pulsations occur at $\epsilon \approx 1.33$ and $\epsilon \approx 1.292$. The upper inset shows Q versus round-trip time for the period-2 solution with additional long period pulsations. The value of ϵ chosen for this case is 1.31 (shown by the arrow).

such solutions can be found numerically. Here, we consider only the simplest cases. Figure 16 is an example of one of the possible bifurcation diagrams leading to double periodic pulsations. It shows the values of the output energy Q as a function of ϵ. For a given set of parameters shown in the lower inset of this figure, the solution is stable at $\epsilon > 1.332$. The system generates the same soliton in each round trip. A bifurcation from stable single period operation to the period doubled solution occurs at around $\epsilon \approx 1.332$. Period-2 solution exists below this value all the way down to $\epsilon = 1.25$. There are two other bifurcations at $\epsilon \approx 1.292$ and $\epsilon \approx 1.33$, limiting a wide area of seemingly chaotic solution, where a diversity of Q values can be obtained rather than two fixed amounts. In fact, in this last region we have a quasiperiodic soliton evolution with two incommensurate periods.

The soliton energy versus the round-trip number for one of these solutions is shown in the upper inset of Fig. 16 by the thick vertical lines. This plot shows clearly the double periodic nature of the solution. After each round trip the Q value jumps from a low (high) value to a high (low) value as it should for period-2 solutions. In addition, the upper and the lower Q values oscillate with a longer period (approximately 18 round trips). The longer period is not exactly a multiple of the round trip time thus creating in Fig. 16 the region of seemingly chaotic motion. The additional period and the amplitude of pulsations vary in the interval between the two bifurcations.

The form of the bifurcation diagram depends on the path in the parameter space that we choose for the simulations. In the case presented in Fig. 16, we fixed all the parameters except one, ϵ. This is one of the easiest ways to change parameters. We can also change two or more parameters simultaneously. Each route creates a specific bifurcation diagram.

Any imaginable combination of long and short periods in the dynamics can be realized with a proper choice of the

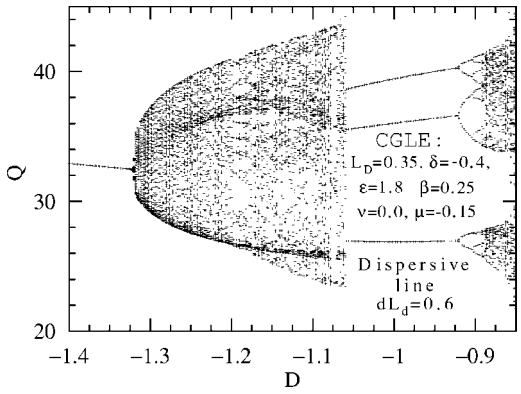

FIG. 17. Bifurcation diagram showing the period tripling bifurcation with additional long period pulsations. The parameters of the simulation are shown in the plot. The vertical line marks the case shown in Fig. 18.

system parameters. New periods appear and disappear at bifurcation points similar to those in Fig. 16. Figure 17 shows another example of bifurcation diagram. This shows a bifurcation from single period to the short period-3 solution; namely, period 1 can be seen clearly in the region below $D \approx -1.32$ and the period-3 solution exists in the interval $-1.05 < D < -0.92$. In between these two regimes, we can see a wide area of soliton evolution with a continuous range of output energies Q. This area corresponds to the quasiperiodic soliton evolution with two incommensurate periods involved in its dynamics. In order to show this we plot in Fig. 18 the soliton energy versus the number of round trips. Each successive pulse is shown by a thick vertical line. This plot shows clearly the double periodic nature of the solution. The line connecting every third point in this plot has a periodicity of around 100 round trips. This longer period is not exactly a multiple of the round-trip time, thus creating in Fig. 17 the region with a continuous range of energies.

The double periodicity is additionally illustrated in Fig. 6(b). This plot is calculated for a different set of parameters but has the same properties: pulsations occur with the com-

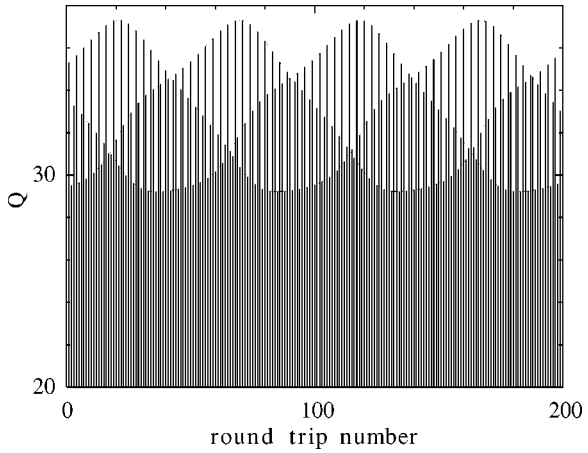

FIG. 18. Period-3 solution with long period soliton pulsations. The parameters of this simulation are the same as in Fig. 17. $D = -1.3$.

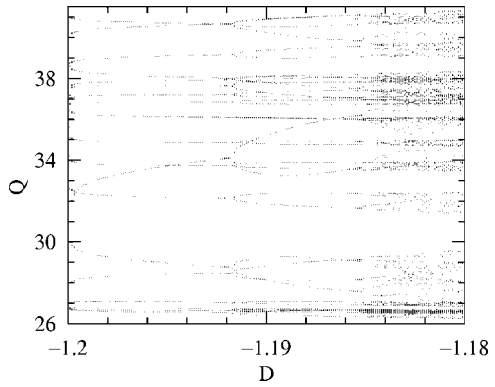

FIG. 19. Part of the bifurcation diagram in Fig. 17 that shows "synchronization."

bination of a period-3 and a long period modulation. The triple limit cycle that is similar to the one shown in Fig. 6(a) is shifted each round trip by a small amount defined by the longer period of pulsations. The final result is this "attractor" which fills the triangular "donut." We stress that the motion is quasiperiodic rather than chaotic in this case.

The new long periods are generally incommensurate with the existing short ones. However, at some range of parameters, the "synchronization" of the two frequencies might happen. Then, a period which is an integer multiple of 3 can be observed. An example of such synchronization can be seen in Fig. 17 in a small window in the region $-1.2<D<-1.19$. The soliton energy takes discrete values rather than an arbitrary amount from the continuous range. This can be seen clearly if we plot the same figure with a higher resolution (see Fig. 19). When more than two frequencies are involved in the pulsations, the sequence of bifurcations can be quite complicated.

To illustrate further the fact that almost any combination of frequencies is possible in pulsations, we give, in Fig. 20, one more example obtained in our numerical simulations. The plot shows a bifurcation diagram from a period-1 solu-

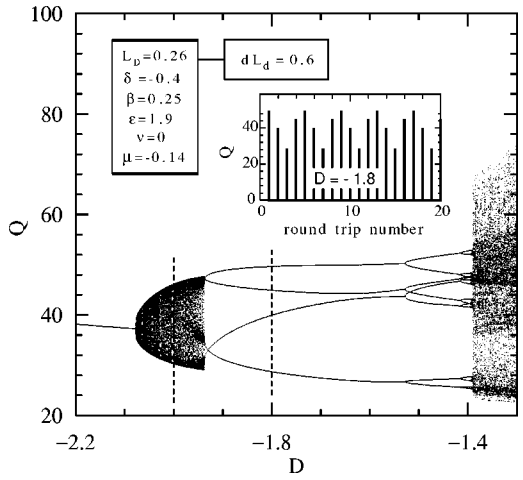

FIG. 20. Bifurcation diagram for the period-4 solution. The inset in the center shows Q versus round-trip number for the period-4 solution at $D=-1.8$. The two boxes at the left upper corner give the parameters of the simulations.

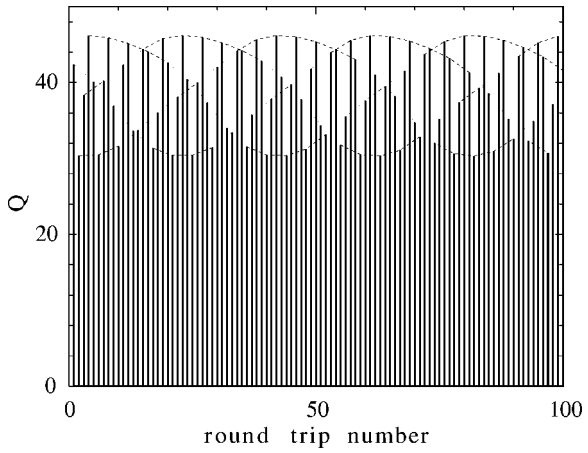

FIG. 21. Period-4 solution with long period pulsations. The parameters of the simulation are the same as in Fig. 20 with $D=-2.0$ (indicated by the left hand dashed line).

tion to a period-4 solution through the combination of a period-4 and a long period pulsation in the same quasiperiodic dynamics. For the values of D below -2.09 the system is in stationary and stable regime producing exactly the same pulse in each round trip. At the values of D in the interval $\approx -1.93<D<\approx -1.52$ the laser produces a period-4 soliton train. The soliton energy versus round-trip time for a particular case $D=-1.8$ is shown in the inset to Fig. 20.

In the intermediate range of D values, the new period appears in addition to the period 4. The two periods are generally incommensurate thus producing the transition region ($\approx -2.09<D<\approx -1.93$) in the bifurcation diagram in Fig. 20. The pulse energy versus the round-trip number for a particular value of D in this region (namely, $D=-2.0$) is shown in Fig. 21. The long period pulsations in this example is ≈ 80. It is remarkable that the transition from period 1 to period 4 does not feature period-2 pulsations as it would happen in the sequence of period doubling bifurcations. This

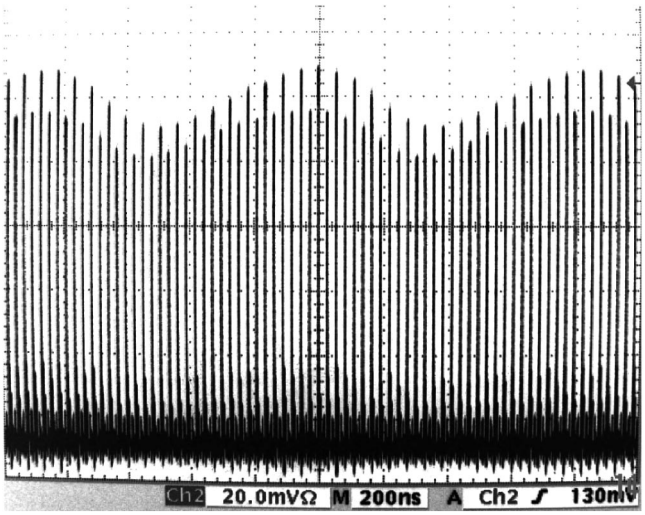

FIG. 22. Experimental oscillogram showing the sequence of laser output pulses with period doubling and long period (≈ 32) pulsations.

example shows that the sequence of bifurcations can be much more involved and depends strongly of the choice of parameters that we fix in simulations.

Experimental observation

Not every dynamics obtained numerically can be easily observed in the experiment. This is related to the fact that some external parameters of the laser system cannot be changed continuously. As a result, some of the regions of parameters cannot be reached in the fixed arrangement of the present setup. Nevertheless, we were successful in observing at least some of the double periodic motions.

For example, using the same procedure as above, we observed period doubling with an additional pulse energy modulation. This experimental result is presented in Fig. 22. Here the same pattern is repeated every ≈ 32 round trips. These long period pulsations exist on the top of the period doubling modulation and generally are incommensurate with period 2. Changing the cavity parameters, we can obtain similar results for the pulse energy modulation with other frequencies combined in the same dynamics. In principle, we can obtain any combination of short and long periods in the pulse energy pulsations.

VII. DISCUSSION

A passively mode-locked fiber laser is a highly nonlinear dissipative system. Moreover, it is a system that has an infinite number of degrees of freedom. As such, it can reveal a variety of interesting dynamics. In particular, the device can serve as a playground for observing nontrivial nonlinear regimes of soliton generation. In some cases, the behavior of these systems has a counterpart in the realm of finite-dimensional systems although there is never a complete correspondence. Some nonlinear phenomena observed in these systems are completely different. To give an example, exploding solitons [10] can be observed only in dissipative systems with an infinite number of degrees of freedom. We have also found that solitons can have chaotic evolution and serve as strange attractors [18].

The pulsating behavior of solitons in dissipative systems is one of the remarkable features that we were able to both predict and observe experimentally. The pulsations are infinite-dimensional analogs of limit cycles. Previous numerical results [10,16] related to soliton pulsations were based on a continuous model which is not always adequate in describing the experimental situation. The explicit introduction of the periodicity in the pulse propagation related to the cavity round-trip time improves the model significantly and makes it closer to the real laser. This improvement allowed us to find both short and long period soliton pulsations in the laser cavity as well as quasiperiodic pulsations with combined frequencies. The latter are examples of more complicated limit cycles.

Surely, the limited number of examples of quasiperiodic motions with two periods in pulsations that we presented in this work do not represent the whole complexity of possible dynamics. Our present study is only the first step in this direction. We can find cases that have three and more periods in the pulsations. Any number of frequencies can be involved in the dynamics. In particular, chaotic pulsations are examples with multiple frequencies. All these complicated phenomena require a more careful study.

An important aspect of the problem is how accurately the model describes an experiment and can it predict new features of pulse generation. In general, comparison of experimental results with simulations is not easy. In most of the cases these comparisons are qualitative rather than quantitative. In this work we made further improvements in laser modeling and used parameter management in order to describe features of soliton generation that are specifically related to the periodicity of the pulse propagation in the laser cavity. This improvement allowed us to describe single and double periodicity in the soliton pulsations.

Last but not least, the additional frequencies can define additional clock speeds in optical devices. If they are synchronized with the round-trip time, these can be quite accurate. We believe that our results can find a variety of practical applications in photonics and optical communications.

VIII. CONCLUSIONS

In conclusion, we observed, both numerically and experimentally, single and double periodic pulsations of solitons generated by a passively mode-locked fiber laser. Additional periods in the laser dynamics appear as bifurcations at certain values of the system parameters.

ACKNOWLEDGMENTS

The work of J.M.S.C. was supported by the MEyC under Contract No. BFM2003-00427. N.A. acknowledges support from the Université de Bourgogne and the Australian Research Council.

[1] J. Herrmann, V. P. Kalosha, and M. Müller, Opt. Lett. **22**, 236 (1997).
[2] A. I. Chernykh and S. K. Turitsyn, Opt. Lett. **20**, 398 (1995).
[3] K. M. Spaulding, D. H. Yong, A. D. Kim, and J. N. Kutz, J. Opt. Soc. Am. B **19**, 1045 (2002).
[4] D. Coté and H. M. van Driel, Opt. Lett. **23**, 715 (1998).
[5] K. Tamura, C. R. Doerr, H. A. Haus, and E. P. Ippen, IEEE Photonics Technol. Lett. **6**, 697 (1994).
[6] F. Ilday, J. Buckley, and F. Wise, *Proceedings of the Nonlinear Guided Waves Conference, Toronto, 2004* (OSA, Washington, DC, 2004), Paper MD9.
[7] Liguo Luo, T. J. Tee, and P. L. Chu, J. Opt. Soc. Am. B **15**, 972 (1998).
[8] G. Sucha, D. S. Chemla, and S. R. Bolton, J. Opt. Soc. Am. B

15, 2847 (1998).
[9] S. Coen, M. Haelterman, Ph. Emplit, L. Delage, L. M. Simohamed, and F. Reynaud, J. Opt. Soc. Am. B **15**, 2283 (1998).
[10] J. M. Soto-Crespo, N. Akhmediev, and A. Ankiewicz, Phys. Rev. Lett. **85**, 2937 (2000).
[11] I. Gabitov, E. G. Shapiro, and S. K. Turitsyn, Phys. Rev. E **55**, 3624 (1997).
[12] J. N. Kutz, P. Holmes, S. G. Evangelides, and J. P. Gordon, J. Opt. Soc. Am. B **15**, 8796 (1998).
[13] K. Tamura, E. P. Ippen, H. A. Haus, and L. E. Nelson, Opt. Lett. **18**, 1080 (1993).
[14] Ph. Grelu, J. Béal, and J. M. Soto-Crespo, Opt. Express **11**, 2238 (2003).
[15] M. J. Lederer, B. Luther-Davies, H. H. Tan, C. Jagadish, N. Akhmediev, and J. M. Soto-Crespo, J. Opt. Soc. Am. B **16**, 895 (1999).
[16] N. Akhmediev, J. M. Soto-Crespo, and G. Town, Phys. Rev. E **63**, 056602 (2001).
[17] F. Gutty, Ph. Grelu, N. Huot, G. Vienne, and G. Millot, Electron. Lett. **37**, 745 (2001).
[18] N. Akhmediev, J. M. Soto-Crespo, and A. Ankiewicz, in *Nonlinear Waves: Classical and Quantum Aspects*, edited by F. Kh. Abdullaev and V. V. Konotop (Kluwer Academic, Dordrecht, 2004), pp. 45–60.